A low cost technique for adding microlasers to a silicon photonic platform

Joan Juvert[a], Iain Eddie[b], Colin J. Mitchell[c], Graham T. Reed[c], James S. Wilkinson[c], Anthony Kelly[a], and Steven L. Neale[a]

[a]School of Engineering, University of Glasgow, 79 Oakfield Ave., Glasgow, United Kingdom
[b]CST Global Ltd., 4 Stanley Boulevard, Hamilton, United Kingdom
[c]Optoelectronics Research Centre, University of Southampton, Southampton, Hampshire, SO17 1BJ, United Kingdom

ABSTRACT

In this paper we report the physical micromanipulation of standard InP telecommunications laser die in a liquid medium by means of optoelectronic tweezers. Optoelectronic tweezers have been shown to use much less optical power than optical tweezers, they do not require a coherent light source to function and the creation of multiple traps is straightforward. These properties make the technique a very good candidate for the massive parallel micromanipulation of optoelectronic components for assembly on a photonic platform. We discuss the positional and orientation accuracy of the optoelectronic tweezers in relation to the alignment requirements for low-loss coupling between the light sources and the other components in a photonic platform. Our experiments indicate that the accuracy is better than 2 µm and 2° for translations and rotations, respectively.

Keywords: optoelectronic tweezers, dielectrophoresis, hybrid integration, silicon photonics

1. INTRODUCTION

In order to overcome the lack of an electrically pumped Si laser that could be monolithically integrated on a silicon photonic circuit, several hybrid strategies have been explored to integrate III-V compounds or Ge on Si. The main advantage of a heterogeneous integration strategy is that, since each component is fabricated separately and then integrated a posteriori, the best technology can be used for each individual component depending on the application.

For long haul applications, a prepackaged III-V laser can be coupled to a silicon photonic chip using optical fibre. This approach allows for the separate optimization of each component, but the large footprint, coupling losses due to reflections at the fibre ends and poor scalability make this approach undesirable for other applications such as on-chip optical interconnects.

An approach better suited for applications that require a small footprint is the heteroepitaxial growth of III-V compounds or Ge on Si.[1] Despite the significant progress that has been made on this area, the large lattice mismatch and the difference in thermal expansion coefficients between the III-V compounds or Ge and the silicon substrate cause performance and reliability issues due to dislocations[2] and strain[3] at the interface.

Wafer bonding is another promising technology. In this case, an InP wafer or unpatterned InP die is bonded to a SOI chip and then further processed to fabricate an array of microlasers. Direct bonding[4], benzocyclobutene (BCB)[5] and metal bonding[6] have been demonstrated. This technique allows a good alignment accuracy and it scales well, since hundreds of lasers can be obtained from a single bonding step. However, the fabrication of systems that require sources at different wavelengths, for instance for wavelength division multiplexing, remains challenging. Furthermore, bonding at the die level involves significant waste of material.

Another approach is to directly integrate individual laser die to the SOI chip, for instance using solder bumps and pick and place tools. The advantages of this approach are that it has a small footprint, a high yield for

Further author information: (Send correspondence to Joan Juvert)
Joan Juvert: E-mail: joan.juvert@glasgow.ac.uk, Telephone: +44 141 330 4793

the individual light sources, and laser die of different wavelengths can be easily integrated together without any compromise in their respective fabrication processes. On the negative side, alignment accuracies are limited by the pick and place tools or mechanical stops, and the positioning of each die individually results in a low throughput that increases the cost and scales poorly for massive integration. Although the coupling efficiency depends on many factors, in general, lateral misalignments in the order of 1 µm would translate to coupling losses of a few dB[7], and sub-micron accuracies would be required for low loss coupling.

In this paper we present a technique to manipulate and place individual semiconductor lasers on a photonic chip using optoelectronic tweezers (OET). This technique could potentially reach the sub-micron accuracies required for low loss coupling. Furthermore, its straightforward parallelization and automation promise a high throughput to drive the costs down. The principle behind OET is light induced dielectrophoresis. Dielectrophoresis (DEP) is the effect by which a polarisable, but otherwise electrically neutral, particle experiences a net force when it occupies a volume where an external electric field gradient exists. An electric field, constant or not, induces a charge separation in the volume of the particle. This charge separation comes from both the in-phase (dielectric constant) and out-of-phase (conductivity related) components of the electrical permittivity. If, in addition, the electric field changes over the volume of the particle, the force exerted on the positive and negative charges will be different and therefore a net force remains. It can be shown[8,9] that, for a spherical particle with polarisation proportional to the electric field, the DEP force can be written as:

$$\vec{F}_{\mathrm{DEP}} = 2\pi r^3 \epsilon_m \Re\left(\frac{\hat{\epsilon}_p - \hat{\epsilon}_m}{\hat{\epsilon}_p - 2\hat{\epsilon}_m}\right)\vec{\nabla}E^2\,, \tag{1}$$

where r is the radius of the particle, ϵ_m the dielectric constant of the medium, and $\hat{\epsilon}_m$ and $\hat{\epsilon}_p$ are the complex permittivities of the medium and the particle, respectively. The term between parentheses is the real part of the Clausius-Mossotti factor. If the permittivity of the particle is higher than that of the surrounding medium, the Clausius-Mossotti factor is positive and the particle is attracted towards increasing field values (same direction as the gradient of the field). If the permittivity of the medium is higher, the Clausius-Mossotti factor is negative and the particle is repelled away from the regions with high electric field (direction opposite to the gradient).

Traditional DEP experiments involve the use of electrodes submerged in a medium. With light induced DEP, a photonductive surface such as a silicon layer is illuminated in certain areas. The conductivity of the silicon will increase in those illuminated areas due to the photogenerated carriers, and this will create a virtual electrode.

OET have been shown to work well for moving microscopic particles with energy densities in the order of $1\,\mathrm{W\,cm^{-2}}$, resulting in traps about 470 times stiffer per mW of light than conventional optical tweezers[10]. Moreover, no coherence is required, and therefore the illumination can be carried out with standard light sources, for instance a commercial projector focused onto the photoconductive surface. Since a computer can be used to send any static or moving light pattern to the projector, the potential for automation and parallelization is quite clear.

In the past, OET have been used successfully to accurately position microdisk lasers[11] as small as 5 µm in diameter, as well as semiconductor nanowires[12] with diameters ranging from 60 to 200 nm. With our present work, we want to study the positional accuracy of OET for the manipulation of standard InP telecommunications laser die with dimensions 250×250 µm^2, and therefore assess the viability of the technique for integration of light sources on a photonic platform.

2. EXPERIMENTAL

The left panel in figure 1 shows a schematic representation of the OET device used for the present work. A 1 µm thick hydrogenated amorphous silicon layer (a-Si:H) is deposited by plasma enhanced chemical vapour deposition (PECVD) on an ITO coated glass slide. The thickness of the ITO coating is 600 nm. A second ITO coated glass slide is used as a top electrode. A closed chamber with a height of 150 µm is created by sticking a piece of double sided tape with a rectangular cut-out in the middle between the top ITO electrode and the a-Si:H. In order to introduce the sample in the chamber, the fluid with the microlasers in suspension is pipetted onto the a-Si:H, within the double sided tape cut-out, before covering with the top electrode.

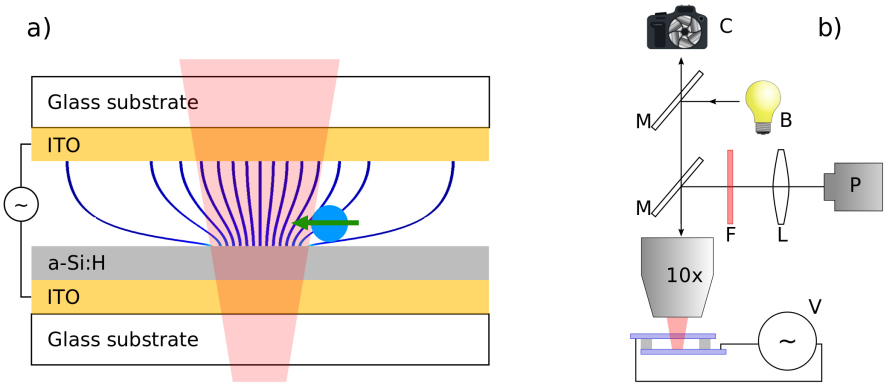

Figure 1. a) Schematic representation of the OET device used in this work. An AC voltage is applied between the two ITO electrodes. The field lines preferentially converge on the illuminated area of the a-Si:H layer. b) Layout of the experimental setup. The elements are (10x) microscope objective; (V) Function generator; (P) Projector; (L) Lens; (F) Long pass filter; (M) 50% mirror; (C) Camera; (B) Lamp for background illumination.

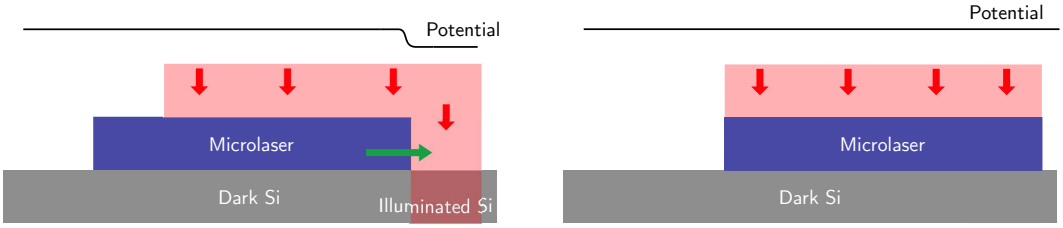

Figure 2. When partially illuminated (left) the dark/illuminated transition at the edge of the microlaser pulls the microlaser until it reaches the opposite edge (right), which effectively cancels the dark/illuminated transition.

The right panel in figure 1 shows the layout of the experimental setup. The sample is biased with a sine waveform from a function generator and imaged by a microscope column. A light source provides global illumination. In order to pattern the virtual electrodes on the a-Si:H surface, the output of a projector is coupled into the microscope column through a lens and a long pass filter. The DEP traps are then projected on the sample just by sending an image, usually a black background with a white pattern, to the projector. This is what makes automation and parallelization so straightforward, since the pattern can range from a static trap to an array of traps that move in an animation. Furthermore, it is a possibility to use an object recognition software to dynamically determine where the traps should be laid out and where they should be moved to.

The semiconductor lasers used for this work are standard InP Fabry-Perot square die with side 250 µm and thickness 100 µm.[13] They are submerged in a KCl solution and pipetted onto the sample. In order to help with their manipulation, a small amount of a surfactant (Tween 20) is used to prevent the die from sticking to the walls of the pipette or the meniscus of the water. The conductivity of the KCl solution with the Tween 20 is $6\,\mathrm{mS\,m^{-1}}$. The electrodes are biased with a sine wave with an amplitude of 30 V peak to peak and frequency 15 kHz.

In order to trap and move the microlasers, a square illuminated area of approximately the same size as the microlasers is projected on the a-Si:H surface. The microlaser is brought to the trap by moving the motorised stage (Prior H101BX ProScan II) where the sample rests. When the edge of the trap contacts the edge of the microlaser, the DEP force pulls the microlaser towards the trap and the die self-aligns to the pattern. Note that the microlaser casts a shadow, which means that, when partially illuminated by the trap, there is a dark/light transition at the edge of the microlaser that pulls it deeper inside the trap until it reaches the opposite edge (see figure 2). That is, the microlaser tries to cover the trap and that brings the self-alignment. See figure 3 for an example of a microlaser being moved and rotated.

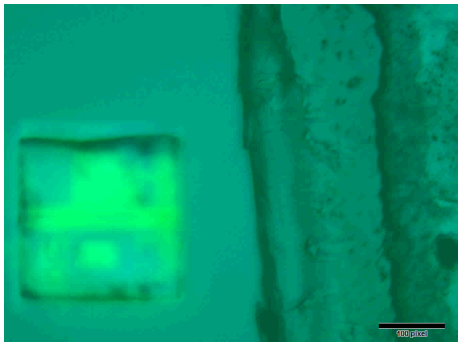

Figure 3. Still of a video showing a semiconductor laser die being moved and rotated. See the video at http://dx.doi.org/doi.number.goes.here.

For our experiments, the square trap is static. In order to move the microlaser within the chamber, we actually move the a-Si:H surface under the die by moving the stage where the device lies while the DEP trap holds the laser in place.

Three tests are carried out. First, the stage is moved in steps of decreasing length. At each step, we measure the position of the microlaser with respect to a fixed reference and compare the measured position to the nominal position of the stage. For simplicity, we keep the movement in a single dimension. In the second test we carry out successive translations of 1 µm. The third test involves the rotation of the microlaser by 45° and back to the initial orientation. Finally, we carry out successive rotations of 1°. For the rotation experiments the stage does not move at all and it is the square illuminated area that is rotated.

The distances and angles are measured from stills extracted from the camera used for imaging the experiment. In our system, the resolution of the camera and the magnification of the microscope objective allow us to measure distances with a resolution of 3 pixels μm^{-1}.

3. RESULTS

Maximum translation velocities in excess of $1\,mm\,s^{-1}$ have been measured for the microlasers, with typical values between 500 and $1000\,\mu m\,s^{-1}$. This allows the microlasers to be moved within a standard $1\,cm^2$ chip area in seconds. Assuming the DEP force and the Sokes drag are the only forces acting on the moving laser die, this corresponds to forces in the order of nN.

Regarding the positional accuracy, figure 4 shows the results for the experiment where the stage is moved in steps of decreasing length. The first step is 5 µm long, followed by 2.5 and finally 1 µm. The left panel plots the absolute position of the microlaser vs. that of the trap. Ideally, we would like the points to fall on the solid line, that is, the position of the microlaser should be the same as that of the trap. The error bars (± 0.5 µm) come from the uncertainty in the measurement of the distance since, as already noted, the resolution of our system is 3 pixels μm^{-1}. Note that, within the error bars, the microlaser moves to the right position in the first step, but lags behind by ≈ 1 µm of the expected position in the following steps.

The right panel in figure 4 compares the travel distance of the microlaser to the travel distance of the trap in each step. It can be observed that our best estimate for the travel distance of the microlaser is very close to the expected value in all the steps. In this case the error bars are ± 1 µm.

Figure 5 shows the results for the test where the stage is moved in successive steps of 1 µm. The left panel shows the absolute position of the microlaser compared to that of the trap. As in the previous experiment, ideally both values should be equal. Considering the error, the microlaser deviates from the expected position in no more than 2 µm in the worst case.

The right panel shows the absolute travel distance in each step. In this case, it should be always around 1 µm. Again, we can see that, once the error is considered, the travel distance would be 3 µm in the worst possible case.

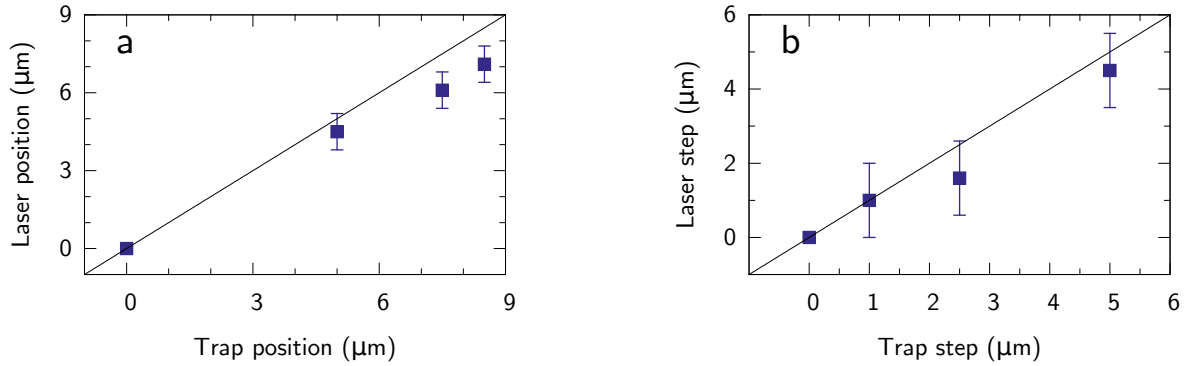

Figure 4. (a) Measured position of the microlaser compared to the position of the trap, for translations of decreasing distance. Ideally the points should fall on the solid line. (b) Absolute value of the distance travelled by the microlaser in each step vs. the translation of the trap.

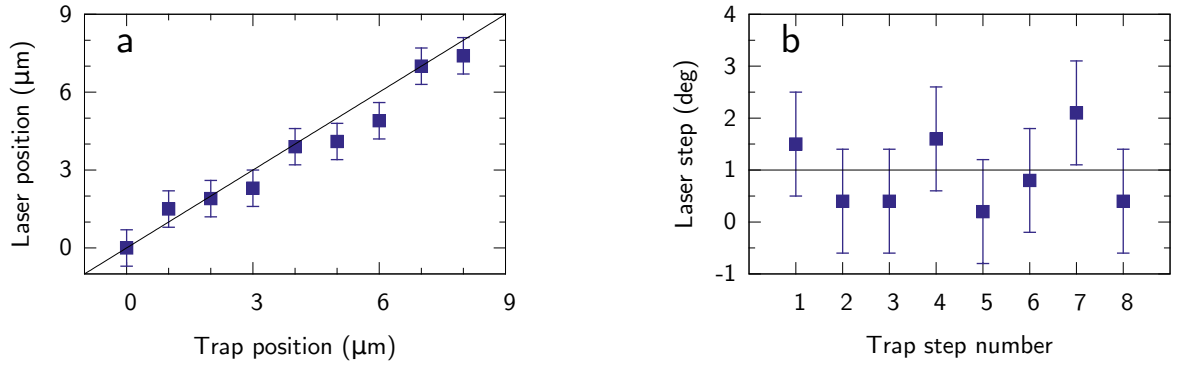

Figure 5. (a) Measured position of the microlaser compared to the position of the trap for successive translations of 1 um. (b) Absolute value of the distance travelled by the microlaser in each step.

An interesting effect is observed in this experiment. Clearly, it looks like the microlaser lags behind the expected position for two steps and then it catches up during the third. This could be due to static friction: over two steps the microlaser accumulates a certain offset with respect to the trap, but static friction with the a-Si:H surface cancels the DEP force that pulls it towards the centre of the trap. According to previous simulations, we expect the force to become stronger with increasing offset.[14] When the offset reaches a certain limit, the DEP force is strong enough to overcome the static friction and pull it back to the right position.

Graphs *a* and *b* in figure 6 show the results for a rotation from 0° to 45° and back to 0°. The rotation is not carried out in a discrete jump, but rather in a continuous movement that takes about 2 s to go from the initial orientation of 0° to the final one of 45°. Graph *a* shows the absolute orientation of the microlaser against that of the trap. The initial orientation of the microlaser is about −2.5°. After the trap rotates to 45° the microlaser matches the final orientation quite well (the error bars of ± 0.5° are hard to see in this scale). When the trap goes back to the original orientation, the microlaser returns to its own original orientation of about −2.5° within the error bars. This initial offset could be explained by the nonuniformity in the light intensity of the square trap due to an imperfect coupling of the projector light into the microscope objective. The nonuniformity of the light intensity would naturally translate to a variable DEP force in different areas of the illuminated region. Graph *b* in figure 6 shows the absolute value of each rotation. Both of them are well above the nominal 45° because the laser die starts and ends the rotation below 0° but matches the intermediate 45° orientation well.

Finally, graphs *c* and *d* in figure 6 show the results corresponding to successive discrete rotations of 1°. Again, the solid line in graph *b* corresponds to the expected ideal values. The *raw* data set corresponds to the measured orientations, and they show clearly the initial offset of the microlaser. The *with offset* data set shows the same

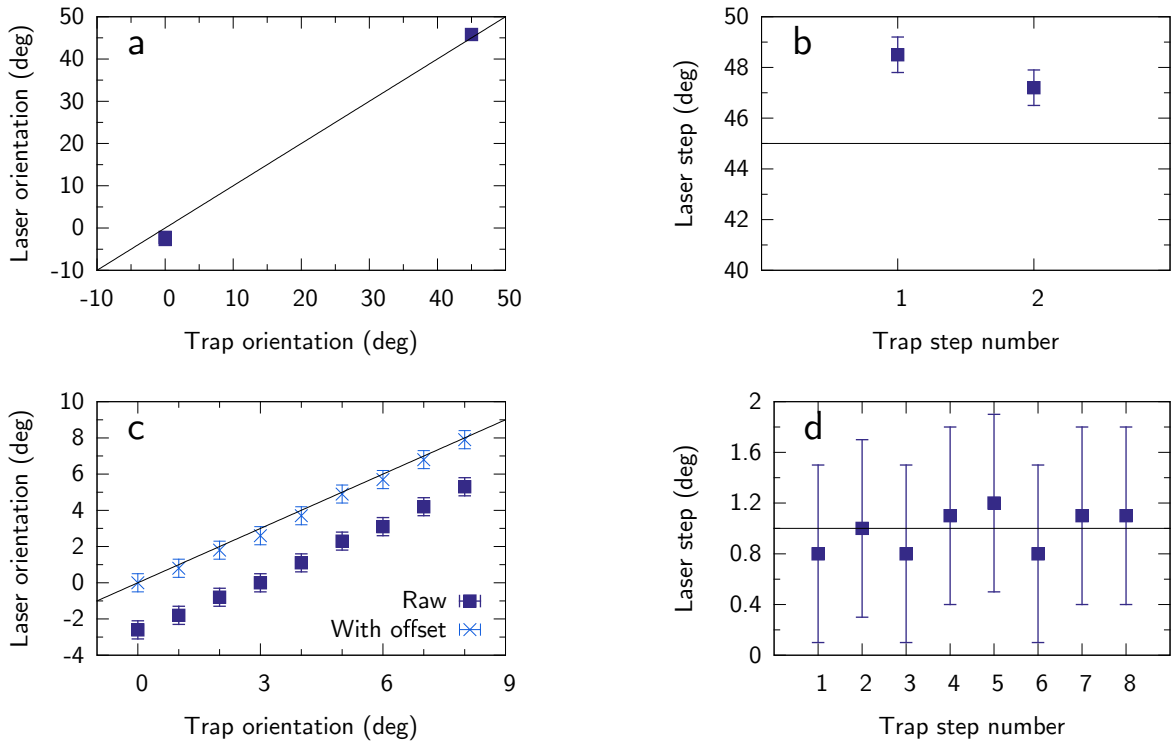

Figure 6. (a) Measured orientation of the microlaser compared to the orientation of the square trap. (b) Absolute value of the rotation amplitude for the two movements (from 0° to 45° and from 45° to 0°). (c) Absolute orientation of the microlaser as a function of the absolute orientation of the trap. The *raw* points are as measured, whereas the *with offset* points are offset in such a way that initial orientation of the microlaser corresponds to 0°. (d) Absolute rotation of the microlaser in each step.

results after adding an offset to the data that cancels the offset in the initial orientation of the microlaser with respect to the trap. The results then follow very well the expected trend. This is confirmed in graph *d*, which shows the absolute rotation amplitude of each step, where we can see that each individual rotation is indeed close to the expected 1° value within the error bars, in this case ± 0.7°.

From the results presented in figures 4 to 6 we can extract an upper bound to the position and orientation accuracies. Considering the limit of the error bars further away from the expected values, we get an accuracy better than 2 µm for the translation and 2° for the orientation.

4. CONCLUSION

Given the upper bound of 2 µm and 2° for translation and orientation accuracies, respectively, the results seem encouraging and justify further study. Improvement of our experimental setup is sure to result in stronger forces, which would improve the accuracy globally, as well as a more uniform DEP force along the edges of the microlaser die, which would positively affect the orientation accuracy in particular. An improvement of the resolution of our measuring system would also provide a more precise assessment of the inaccuracies themselves. Given our current error bars, it is likely we are significantly underestimating the best possible accuracy. Further study of the accuracy as a function of the size of the trap would also allow us to optimize the system.

ACKNOWLEDGMENTS

This work is funded by the innovation fund from the EPSRC Silicon Photonics for Future Systems programme grant EP/L00044X/1. Reed is a Royal Society Wolfson Research Merit Award holder. He is grateful to the Wolfson Foundation and the Royal Society for funding of the award.

REFERENCES

[1] Kawanami, H., "Heteroepitaxial technologies of III-V on Si," *Solar Energy Materials and Solar Cells* **66**, 479–486 (2001).

[2] Samonji, K., Yonezu, H., Takagi, Y., Iwaki, K., Ohshima, N., Shin, J. K., and Pak, K., "Reduction of threading dislocation density in InP-on-Si heteroepitaxy with strained short-period superlattices," *Applied Physics Letters* **69**(1), 100 (1996).

[3] Yamaguchi, M., Sugo, M., and Itoh, Y., "Misfit stress dependence of dislocation density reduction in GaAs films on Si substrates grown by strained-layer superlattices," *Applied Physics Letters* **54**(25), 2568–2570 (1989).

[4] Pasquariello, D. and Hjort, K., "Plasma-assisted InP-to-Si low temperature wafer bonding," *IEEE Journal of Selected Topics in Quantum Electronics* **8**(1), 118–131 (2002).

[5] Roelkens, G., Liu, L., Liang, D., Jones, R., Fang, A., Koch, B., and Bowers, J., "III-V/silicon photonics for on-chip and intra-chip optical interconnects," *Laser and Photonics Reviews* **4**(6), 751–779 (2010).

[6] Tanabe, K., Guimard, D., Bordel, D., Iwamoto, S., and Arakawa, Y., "Electrically pumped 1.3 microm room-temperature InAs/GaAs quantum dot lasers on Si substrates by metal-mediated wafer bonding and layer transfer.," *Optics express* **18**(10), 10604–10608 (2010).

[7] Luff, B., Feng, D., Lee, D., and Qian, W., "Hybrid silicon photonics for low-cost high-bandwidth link applications," *Advances in Optical Technologies* **2008**, 1–6 (2008).

[8] Pohl, H. A., [*Dielectrophoresis: the behavior of neutral matter in nonuniform electric fields*], Cambridge University Press, Cambridge (1978).

[9] Jones, T. B., [*Electromechanics of particles*], Cambridge University Press, Cambridge (1995).

[10] Neale, S. L., Mazilu, M., Wilson, J. I. B., Dholakia, K., and Krauss, T. F., "The resolution of optical traps created by Light Induced Dielectrophoresis (LIDEP).," *Optics express* **15**(20), 12619–12626 (2007).

[11] Tien, M. C., Ohta, A. T., Yu, K., Neale, S. L., and Wu, M. C., "Heterogeneous integration of InGaAsP microdisk laser on a silicon platform using optofluidic assembly," *Applied Physics A: Materials Science and Processing* **95**, 967–972 (2009).

[12] Neale, S. L., Fan, Z., Ohta, a. T., Jamshidi, a., Valley, J. K., Hsu, H. Y., Javey, a., and Wu, M. C., "Optofluidic Assembly of Red / Blue / Green Semiconductor Nanowires," *Assembly* , 1–2 (2009).

[13] Cantú, H. I., McKee, A., Eddie, I., and Kelly, A. E., "Parametric study of 1310 nm ridge waveguide AlGaInAs-InP semi-conductor laser dynamics," *IET Optoelectronics* **9**(6), 341–347 (2015).

[14] Neale, S. L., Ohta, A. T., Hsu, H.-Y., Valley, J. K., Jamshidi, A., and Wu, M. C., "Trap profiles of projector based optoelectronic tweezers (OET) with HeLa cells.," *Optics express* **17**(7), 5232–9 (2009).